NANO LETTERS

Letter

pubs.acs.org/NanoLett

Structure-Sensitive CO_2 Electroreduction to Hydrocarbons on Ultrathin 5-fold Twinned Copper Nanowires

Yifan Li,[†,§] Fan Cui,[†,§] Michael B. Ross,[†] Dohyung Kim,[‡,⊥] Yuchun Sun,[†] and Peidong Yang*[,†,‡,§,∥,⊥]

[†]Department of Chemistry and [‡]Department of Materials Science and Engineering, University of California, Berkeley, California 94720, United States

[§]Chemical Sciences Division and [∥]Materials Sciences Division, Lawrence Berkeley National Laboratory, Berkeley, California 94720, United States

[⊥]Kavli Energy Nanosciences Institute, Berkeley, California 94720, United States

Supporting Information

ABSTRACT: Copper is uniquely active for the electrocatalytic reduction of carbon dioxide (CO_2) to products beyond carbon monoxide, such as methane (CH_4) and ethylene (C_2H_4). Therefore, understanding selectivity trends for CO_2 electrocatalysis on copper surfaces is critical for developing more efficient catalysts for CO_2 conversion to higher order products. Herein, we investigate the electrocatalytic activity of ultrathin (diameter ~20 nm) 5-fold twinned copper nanowires (Cu NWs) for CO_2 reduction. These Cu NW catalysts were found to exhibit high CH_4 selectivity over other carbon products, reaching 55% Faradaic efficiency (FE) at −1.25 V versus reversible hydrogen electrode while other products were produced with less than 5% FE. This selectivity was found to be sensitive to morphological changes in the nanowire catalyst observed over the course of electrolysis. Wrapping the wires with graphene oxide was found to be a successful strategy for preserving both the morphology and reaction selectivity of the Cu NWs. These results suggest that product selectivity on Cu NWs is highly dependent on morphological features and that hydrocarbon selectivity can be manipulated by structural evolution or the prevention thereof.

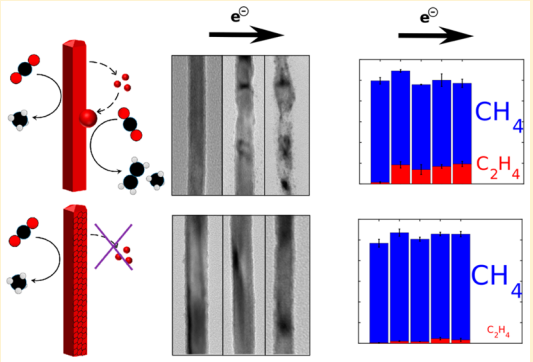

KEYWORDS: *5-fold twinned nanowires, carbon dioxide reduction, electrocatalysis, selectivity, graphene oxide, morphological evolution*

Electrocatalytic CO_2 conversion to value-added products is an attractive means for mitigating the unsustainable rise in anthropogenic CO_2 emissions. Coupled with renewably generated electricity, a CO_2 electrolyzer provides simultaneous carbon fixation and renewable energy storage.[1−3] Many catalytic studies in recent years have refined the electrocatalytic conversion of CO_2 to CO, increasing its commercial viability by reducing overpotential and increasing current density.[4−9] However, an efficient electrocatalyst for the conversion of CO_2 to higher order products beyond CO has yet to be developed. Though several metals and metal alloys are known to produce small quantities of higher order products at high overpotentials,[10] only copper has been shown to do so with appreciable activity.[11] Controlling product selectivity, meanwhile, remains a challenge using a copper foil catalyst.[12] Comparisons between the same copper foil under various chemical treatments, creating different nanostructures, resulted in remarkable differences in product selectivity.[13] Therefore, understanding how to manipulate selectivity on the copper surface via nanostructure is critical for the development of new selective catalysts.

Nanoscale catalysts present considerable advantages compared to their bulk counterparts, including higher surface areas and a high density of low-coordination, high-activity catalytic sites. Indeed, nanostructuring has been shown to improve activity for a variety of catalytic materials, primarily by improving turnover (i.e., partial current density toward products) and/or selectivity at lower overpotentials.[5,6,8,14] Typically, nanostructured catalyst films are produced through chemical and electrochemical treatments of copper foil, resulting in drastically improved selectivity and activity for high-value products like ethylene.[15−19] However, the mechanism and origin for the improved activity is poorly understood, requiring a platform with precise control over size, shape, and composition. Colloidal nanomaterial synthesis provides a means to synthesize such well-defined electrocatalysts but has only recently been explored for studying CO_2 electrocatalysis. For example, several recent works have conducted investigations into electrocatalytic CO_2 reduction on various colloidal Cu nanomaterials.[20−24]

One-dimensional nanowires (NWs) are an especially intriguing class of nanostructure for CO_2 electrocatalysis. Previous work on CO_2 reduction on Cu NWs have shown improved performance on wires with diameters ranging from 100 nm to

Received: December 20, 2016
Revised: January 12, 2017
Published: January 17, 2017

DOI: 10.1021/acs.nanolett.6b05287
Nano Lett. 2017, 17, 1312−1317

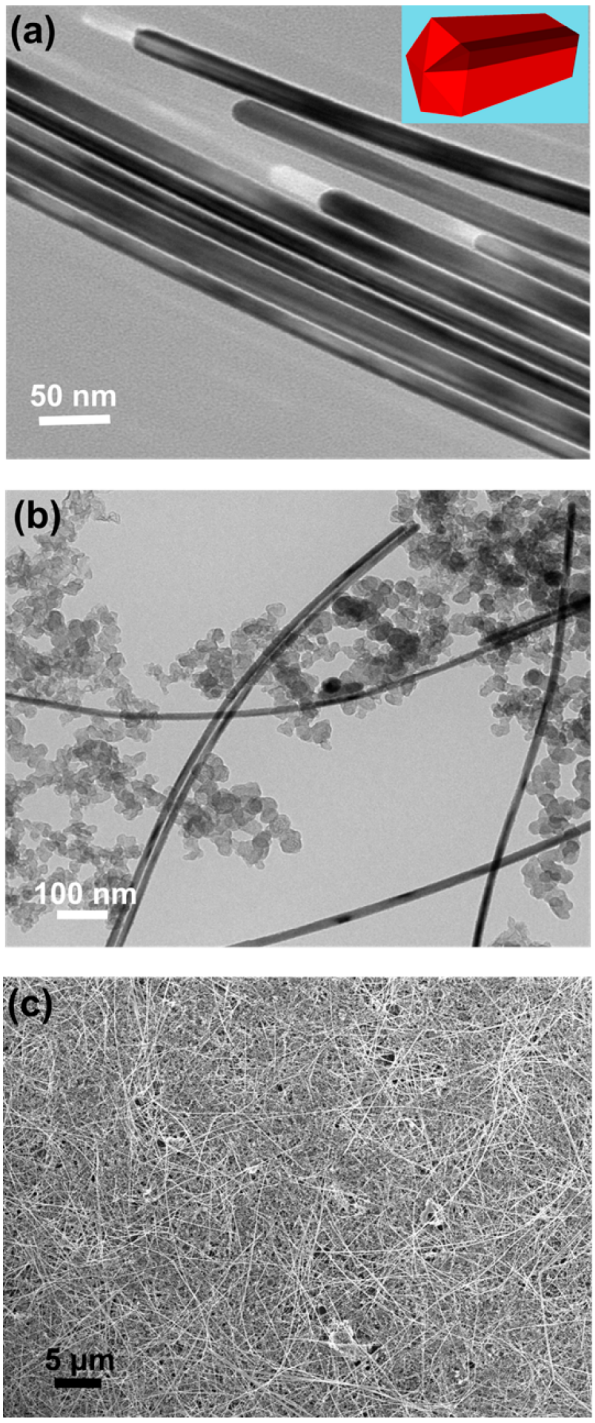

Figure 1. Synthesis of 5-fold twinned copper nanowires. (a) TEM image of bare wires, around 20 nm in diameter, before loading. Inset: illustration of the 5-fold twinned structure, showing a high proportion of low-coordination edge sites (dark red) brought about by 5-fold twin boundaries. (b) TEM micrograph of Cu NWs loaded on carbon black with 20 wt % loading. (c) SEM micrograph of the CuNW/CB catalyst dispersed on a glassy carbon surface, used as the electrode for electrochemical experiments.

several microns.[25−27] However, the catalytic activity of ultrathin Cu NWs with well-defined twin boundary edges, has yet to be investigated. The presence of low-coordination edge sites on an ultrathin nanowire presents a catalytic surface with potential for high activity and unique selectivity due to the difference in intermediate binding on low-coordination sites. Zhu et al. have previously shown markedly higher CO selectivity on ultrathin Au NWs, which they attribute by DFT calculations to enhanced intermediate binding on edge sites.[7] In addition, the presence of grain boundaries in copper nanoparticles have been shown to directly promote CO electroreduction to multicarbon products.[28] Thus, studying the catalytic influence of the ultrathin NW morphology using ultrathin Cu NWs[29] is highly relevant to CO_2 electroreduction.

Another point of interest for the nanowire geometry is its ability to be modified by graphene oxide wrapping. Previous work on copper nanoparticles has shown a tendency for particles to sinter at high bias, potentially as a result of electrochemical migration or copper dissolution and redeposition.[20] We have recently demonstrated that ultrathin Cu NWs can be wrapped with a thin reduced graphene oxide (rGO) shell to enhance their structural stability.[30] The wrapped Cu NW system provides an intriguing platform for studying the catalytic effects of morphological change and its prevention. Therefore, we set out to investigate how well-faceted Cu NW surfaces change over electrolysis and whether the electrocatalytic activity changes in conjunction. Subsequently, we wished to study whether rGO-wrapping could preserve the Cu NW morphology under electrolytic conditions and whether such a strategy simultaneously preserves electrocatalytic properties hypothesized to be morphology-dependent.

Figure 1a shows a transmission electron microscope (TEM) micrograph of the as-synthesized bare Cu NWs, which have a diameter of approximately 20 nm. The 5-fold-twinned structure of the NWs with well-defined edges is illustrated in the inset. To test their catalytic behavior toward CO_2 reduction, freshly made Cu NWs were loaded onto carbon black (CB) to make a 20 wt % CuNW/CB catalyst suspension in hexanes, as confirmed by TEM (Figure 1c). This suspension was pasted onto glassy carbon plates to make a working electrode, which scanning electron microscopy (SEM) revealed to be a conductive mesh of Cu wires and carbon black (Figure 1d). Direct loading of the Cu NW catalyst onto the glassy carbon substrate was also explored. It was found that while the catalytic activities between the CuNW/GC and CuNW/CB/GC electrodes were comparable, the latter formulation was more mechanically stable. Without carbon black, the Cu NWs visibly disappear from the electrode after 1 C of electrolysis (Figure S1).

Thereafter, the CuNW/CB catalyst was tested over a range of potentials for catalytic activity, which showed a marked selectivity for methane at potentials more negative than −1.1 V versus reversible hydrogen electrode (RHE) (Figure 2a). Faradaic efficiencies (FEs) for methane at the potentials tested reached a maximum of 55% at −1.25 V versus RHE. Notably, while polycrystalline copper has frequently been reported to produce a spread of C1 and C2 products at potentials below −1 V versus RHE, the CuNW catalyst produces nearly exclusively methane among the carbon-derived products. In fact, in the potential region tested spanning 600 mV, neither carbon monoxide (CO) nor ethylene (C_2H_4) exceed 5% of all products, while formate is only substantially produced at potentials more positive than −1 V versus RHE. Total FEs consistently reached 90−100% at potentials where methane was produced selectively (Figure 2b), suggesting the successful detection of all major products at methane-selective potentials.

To more aptly gauge the activity of the catalyst toward methane, the partial current density toward methane (j_{CH4}) was also calculated and compared with a reference polycrystalline

DOI: 10.1021/acs.nanolett.6b05287
Nano Lett. 2017, 17, 1312−1317

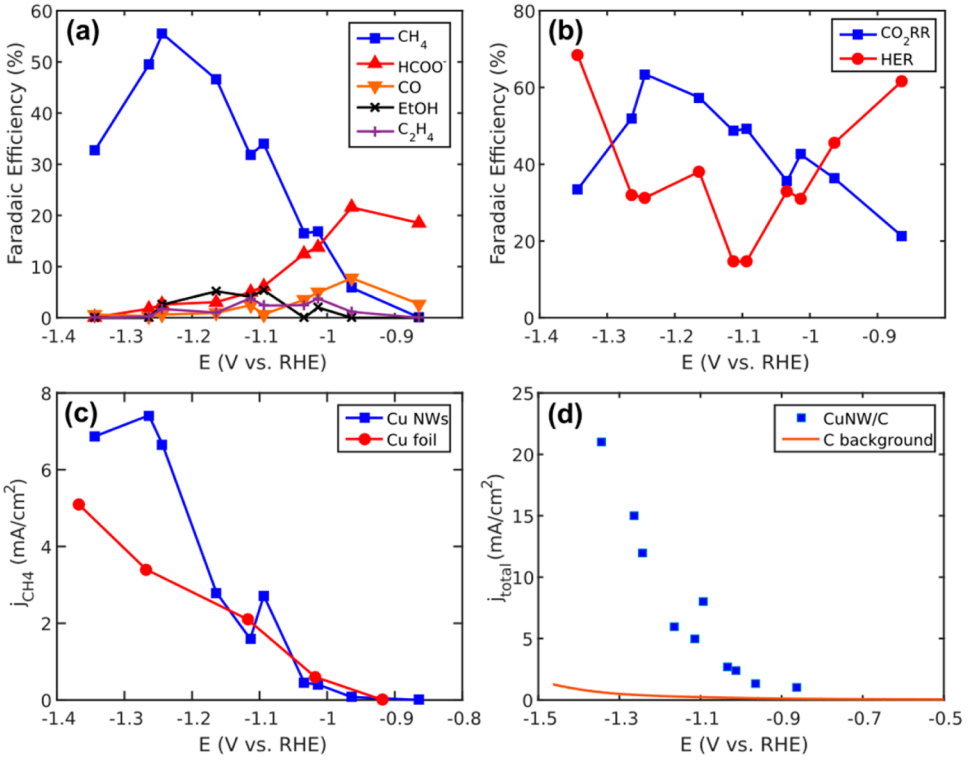

Figure 2. Cu NW initial electrocatalytic activity and selectivity. (a) Products of CO_2 reduction, showing the prevalence of CH_4 at high bias over other products (CO, C_2H_4, formate, and ethanol). Acetate, methanol, and *n*-propanol were detected in trace. (b) Total FE of CO_2RR and the competing reaction, hydrogen evolution (HER). (c) Partial current density toward methane of the Cu NW catalyst compared with a cleaned polycrystalline copper foil, showing the increased activity at more negative potential. (d) Total geometric current density over the range of potentials, compared to background current from the glassy carbon substrate with bare carbon black loaded. Initial activity electrocatalytic tests were conducted over the potential range of −0.85 to −1.35 V versus RHE in 0.1 M $KHCO_3$ over 1 C of passed charge.

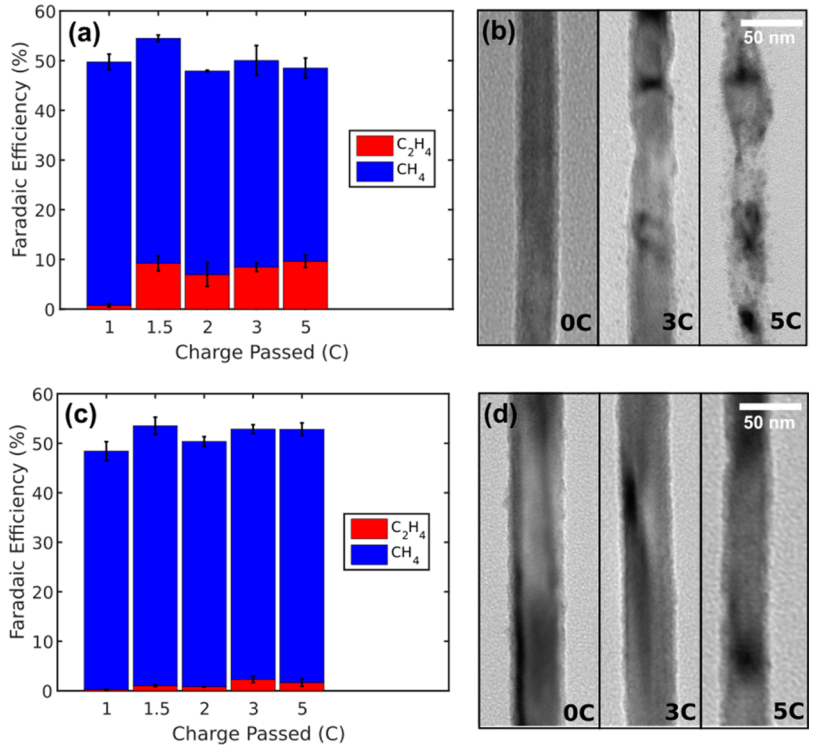

Figure 3. Electrocatalytic and morphological evolution of the Cu NW catalyst. (a) Rapid onset of C_2H_4 formation with a concurrent decrease in CH_4 activity after the first Coulomb of electrolysis. (b) Representative Cu NWs imaged under TEM after a given amount of charge passed, showing visible fracturing and the formation of small Cu NPs. (c,d) Analogous electrocatalytic and morphological characterization for the rGO-Cu NW catalyst, showing preservation of selectivity as well as morphology.

DOI: 10.1021/acs.nanolett.6b05287
Nano Lett. 2017, 17, 1312−1317

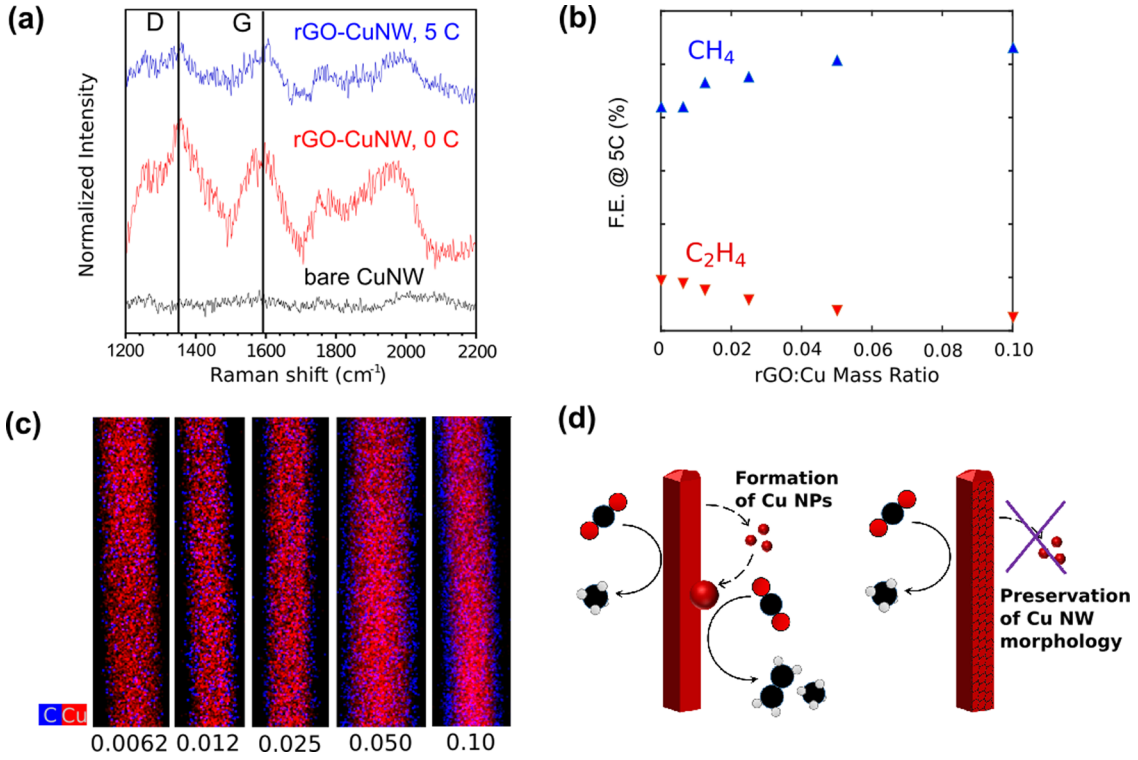

Figure 4. Evidence for the protective role of reduced graphene oxide. (a) From bottom to top, Raman spectra of bare CuNWs, GO-wrapped CuNWs before electrolysis, and rGO-wrapped CuNWs after electrolysis. The D and G peaks attributable to graphene oxide are indicated, showing its presence and retention after 5 C electrolysis. (b) CH_4 and C_2H_4 selectivity at 5 C on Cu NWs wrapped with varying amounts of GO used in preparation, showing preservation of CH_4 selectivity with increasing rGO wrapping. (c) EDS mapping showing the increasing presence of carbon species attributed to graphene oxide surrounding the wires as the amount of GO used in preparation of the catalyst is increased. (d) Scheme for the correlation between morphology and selectivity observed in this study. C_2H_4 onset is thought to be due to the transformation of NW edge sites to small NPs deposited on the surface (left), which rGO wrapping prevents (right).

Cu foil. The corresponding measured j_{CH4} values for the Cu foil are within range of previous results.[20,31] Although j_{CH4} for the two catalysts is comparable at lower overpotentials, the CuNW-loaded electrode achieves partial current to methane double that of Cu foil past −1.2 V versus RHE (Figure 2c). The background current contributed by the same mass of carbon black on glassy carbon was minimal even at the most negative potentials applied (Figure 2d), confirming that the measured j_{CH4} is due to the Cu NW catalyst.

Electrocatalytic activity was also measured with varying amounts of passed charge before product measurement. Strikingly, the selectivity of the catalyst was observed to change with increasing charge passed at −1.25 V versus RHE (Figure 3a). Coulomb-by-Coulomb analysis of the activity evolution shows that the hydrocarbon selectivity shifts from almost entirely CH_4 to higher production of C_2H_4 over the course of 5 C passed. Other products (such as CO, H_2, and liquid products) were not observed to change substantially over this period (Figure S4). The shift in selectivity appears shortly after the first Coulomb passed. This change in activity suggests that the catalyst is rapidly evolving at potentials relevant to hydrocarbon formation. TEM confirms that the morphology of the catalyst changes as a function of charge passed during electrolysis. For example, Figure 3b shows that after 1 C, the wire morphology begins to degrade, resulting in particle formation, wire bundling, disintegration, and fracturing.

To investigate whether the structure of a wire could be preserved, thereby also preserving the CO_2 electrocatalytic selectivity for methane, we studied the electrocatalytic properties of rGO-wrapped copper nanowires. Wrapped Cu NWs were loaded on carbon black and glassy carbon under identical loading conditions to the bare Cu NWs and tested for CO_2 electrocatalytic activity. Figure 3c shows analogous electrocatalytic and TEM results to Figure 3a,b using the rGO-wrapped CuNWs/CB catalyst. In contrast with the bare wires, rGO-wrapped wires preserve their selectivity for methane over ethylene for up to 5 C passed. Simultaneously, the wires show no morphological evolution under TEM. Typical single wires were selected for Figure 3b,d to highlight the morphological difference between rGO-CuNWs and bare CuNWs under bias. TEM micrographs imaged at varying points of the electrolysis for each catalyst in the ensemble have been included in the Supporting Information (Figures S5, S6).

To verify the presence of rGO on the surface of the catalyst, we conducted Raman spectroscopy on the rGO-CuNW catalyst pre- and postelectrolysis. Both before and after 5 C of electrolysis, Raman spectra of the rGO-CuNW exhibit the characteristic D and G bands of GO or rGO (Figure 4a).[32] For comparison, a Raman spectrum of the unwrapped wires is shown, which exhibits no peaks attributed to rGO. Wrapped Cu NWs with varying amounts of rGO were then used as electrodes for CO_2 electroreduction to probe whether increasing rGO wrapping better preserves electrocatalytic selectivity. Figure 4b shows that increasing the amount of rGO wrapping on the wires increasingly preserves high methane selectivity over ethylene over 5 C of electrolysis. Energy dispersive X-ray spectroscopic (EDS) mapping of carbon further verifies the presence of rGO on the surface of the Cu NWs and that

DOI: 10.1021/acs.nanolett.6b05287
Nano Lett. 2017, 17, 1312−1317

increasing the mass ratio of GO to copper used in the preparation qualitatively increases the amount of rGO wrapping in the final catalyst (Figure 4c).

Taken together, these data suggest that nanowire-specific structural features, such as edge sites, are responsible for stabilizing intermediates that lead to improved methane selectivity in CO_2 electroreduction. The five twin boundaries on the ultrathin Cu NW present a unique active site for stabilizing CO_2 intermediates, which previous DFT studies have suggested enhance methane formation.[33] As the wires evolve under bias, the well-defined twin boundaries degrade, while Cu nanoparticles simultaneously nucleate on the NW surface and create a variety of ill-defined active sites. The shift in selectivity from methane to ethylene shown here is approximately 10% FE, such that the final ethylene selectivity at −1.25 V versus RHE is comparable to previous reports of ethylene selectivity for polycrystalline copper foil.[31] However, it is difficult to identify the active site of the evolved catalyst, as it consists of a diverse array of roughened wires, small particles, and likely some remaining twin boundaries, all of which exhibit distinct catalytic selectivity. The tunability of electrocatalytic selectivity with an amount of rGO directly supports the role of rGO in preserving structure and selectivity. Figure 4d summarizes the effects of changing and preserving morphology on electrocatalytic selectivity: copper nanoparticle formation and edge loss shifts the morphology from high-density methane-selective sites to a mix of methane-selective and mixed-selectivity sites. Introducing rGO as a wrapping layer impedes nanoscale structural change and prevents the loss of methane-selective sites.

We have shown that one-dimensional ultrathin 5-fold twinned copper nanowires exhibit high methane selectivity for CO_2 electrocatalysis relative to other carbon products. The origin of the methane selectivity is likely due to the presence of a high density of edge sites owing to the twin boundaries. Furthermore, the morphology of these wires and their electrocatalytic selectivity evolve, losing methane selectivity in favor of ethylene formation. We posit that the change in electrocatalytic selectivity is due to the change in morphology, a claim directly supported by the observation that rGO wrapping simultaneously preserves morphology and methane selectivity over the same electrocatalytic conditions. This study highlights the importance of manipulating nanostructural transformations of copper electrocatalysts under conditions relevant to CO_2 electroreduction, a topic that merits in-depth future study. Moreover, it demonstrates the employment of rGO wrapping as a strategy for electrocatalyst stabilization, a method that may be explored for other catalysts in which morphological change is evident.

■ ASSOCIATED CONTENT

Supporting Information

The Supporting Information is available free of charge on the ACS Publications website at DOI: 10.1021/acs.nanolett.6b05287.

Synthesis and electrochemical methods, full product distribution, additional imaging and electrochemical tests (PDF)

■ AUTHOR INFORMATION

Corresponding Author

*E-mail: p_yang@berkeley.edu.

ORCID

Yifan Li: 0000-0003-2146-2266

Fan Cui: 0000-0003-3394-8095

Peidong Yang: 0000-0003-4799-1684

Author Contributions

Y.L., F.C., and P. Y. designed the experiments and wrote the paper. F.C. and Y.S. synthesized copper nanowires and graphene oxide wrapped nanowires. Y.L. and F.C. carried out structural characterization. Y.L. fabricated the electrodes and conducted all electrocatalytic tests. M.B.R. conducted the Raman spectroscopy. All authors discussed the results and commented on the manuscript. Y.L. and F.C. contributed equally to this work.

Notes

The authors declare no competing financial interest.

■ ACKNOWLEDGMENTS

This work was supported by Director, Office of Science, Office of Basic Energy Sciences, Chemical Sciences, Geosciences, and Biosciences Division, of the U.S. Department of Energy under Contract No. DE-AC02-05CH11231, FWP No. CH030201 (Catalysis Research Program). We thank the imaging facilities at the National Center for Electron Microscopy (NCEM) at the Molecular Foundry and the NMR facility of the College of Chemistry, University of California, Berkeley. Work at the NCEM was supported by the Office of Science, Office of Basic Energy Sciences, of the U.S. Department of Energy under Contract No. DE-AC02-05CH11231. M.B.R. gratefully acknowledges the Canadian Institute for Advanced Research for funding. D.K. acknowledges support from the Samsung Scholarship.

■ REFERENCES

(1) White, J. L.; Baruch, M. F.; Pander, J. E.; Hu, Y.; Fortmeyer, I. C.; Park, J. E.; Zhang, T.; Liao, K.; Gu, J.; Yan, Y.; Shaw, T. W.; Abelev, E.; Bocarsly, A. B. *Chem. Rev.* **2015**, *115*, 12888−12935.

(2) Kim, D.; Sakimoto, K. K.; Hong, D.; Yang, P. *Angew. Chem., Int. Ed.* **2015**, *54*, 3259−3266.

(3) Kondratenko, E. V.; Mul, G.; Baltrusaitis, J.; Larrazabal, G. O.; Perez-Ramirez, J. *Energy Environ. Sci.* **2013**, *6*, 3112.

(4) Rosen, B. A.; Salehi-Khojin, A.; Thorson, M. R.; Zhu, W.; Whipple, D. T.; Kenis, P. J. A.; Masel, R. I. *Science* **2011**, *334*, 643−644.

(5) Lu, Q.; Rosen, J.; Zhou, Y.; Hutchings, G. S.; Kimmel, Y. C.; Chen, J. G.; Jiao, F. *Nat. Commun.* **2014**, *5*, 3242.

(6) Kim, D.; Resasco, J.; Yu, Y.; Asiri, A. M.; Yang, P. *Nat. Commun.* **2014**, *5*, 4948.

(7) Zhu, W.; Zhang, Y. J.; Zhang, H.; Lv, H.; Li, Q.; Michalsky, R.; Peterson, A. A.; Sun, S. *J. Am. Chem. Soc.* **2014**, *136*, 16132−16135.

(8) Chen, Y.; Li, C. W.; Kanan, M. W. *J. Am. Chem. Soc.* **2012**, *134*, 19969−19972.

(9) Liu, M.; Pang, Y.; Zhang, B.; De Luna, P.; Voznyy, O.; Xu, J.; Zheng, X.; Dinh, C. T.; Fan, F.; Cao, C.; de Arquer, F. P. G.; Safaei, T. S.; Mepham, A.; Klinkova, A.; Kumacheva, E.; Filleter, T.; Sinton, D.; Kelley, S. O.; Sargent, E. H. *Nature* **2016**, *537*, 382−386.

(10) Kuhl, K. P.; Hatsukade, T.; Cave, E. R.; Abram, D. N.; Kibsgaard, J.; Jaramillo, T. F. *J. Am. Chem. Soc.* **2014**, *136*, 14107−14113.

(11) Hori, Y. In *Modern Aspects of Electrochemistry*; Vayenas, C., White, R., Gamboa-Aldeco, M., Eds.; Springer: New York, 2008; pp 89−189.

(12) Gattrell, M.; Gupta, N.; Co, A. *J. Electroanal. Chem.* **2006**, *594*, 1−19.

(13) Tang, W.; Peterson, A. A.; Varela, A. S.; Jovanov, Z. P.; Bech, L.; Durand, W. J.; Dahl, S.; Nørskov, J. K.; Chorkendorff, I. *Phys. Chem. Chem. Phys.* **2012**, *14*, 76−81.

DOI: 10.1021/acs.nanolett.6b05287
Nano Lett. 2017, 17, 1312−1317

(14) Zhang, S.; Kang, P.; Meyer, T. J. *J. Am. Chem. Soc.* **2014**, *136*, 1734−1737.
(15) Li, C. W.; Kanan, M. W. *J. Am. Chem. Soc.* **2012**, *134*, 7231−7234.
(16) Kas, R.; Kortlever, R.; Yılmaz, H.; Koper, M. T. M.; Mul, G. *ChemElectroChem* **2015**, *2*, 354−358.
(17) Ren, D.; Deng, Y.; Handoko, A. D.; Chen, C. S.; Malkhandi, S.; Yeo, B. S. *ACS Catal.* **2015**, *5*, 2814−2821.
(18) Roberts, F. S.; Kuhl, K. P.; Nilsson, A. *Angew. Chem., Int. Ed.* **2015**, *54*, 5179−5182.
(19) Mistry, H.; Varela, A. S.; Bonifacio, C. S.; Zegkinoglou, I.; Sinev, I.; Choi, Y.; Kisslinger, K.; Stach, E. A.; Yang, J. C.; Strasser, P.; Cuenya, B. R. *Nat. Commun.* **2016**, *7*, 12123.
(20) Manthiram, K.; Beberwyck, B. J.; Alivisatos, A. P. *J. Am. Chem. Soc.* **2014**, *136*, 13319−13325.
(21) Baturina, O. A.; Lu, Q.; Padilla, M. A.; Xin, L.; Li, W.; Serov, A.; Artyushkova, K.; Atanassov, P.; Xu, F.; Epshteyn, A.; Brintlinger, T.; Schuette, M.; Collins, G. E. *ACS Catal.* **2014**, *4*, 3682−3695.
(22) Reske, R.; Mistry, H.; Behafarid, F.; Roldan Cuenya, B.; Strasser, P. *J. Am. Chem. Soc.* **2014**, *136*, 6978−6986.
(23) Loiudice, A.; Lobaccaro, P.; Kamali, E. A.; Thao, T.; Huang, B. H.; Ager, J. W.; Buonsanti, R. *Angew. Chem., Int. Ed.* **2016**, *55*, 5789−5792.
(24) Wang, Z.; Yang, G.; Zhang, Z.; Jin, M.; Yin, Y. *ACS Nano* **2016**, *10*, 4559−4564.
(25) Ma, M.; Djanashvili, K.; Smith, W. A. *Angew. Chem., Int. Ed.* **2016**, *55*, 6680−6684.
(26) Raciti, D.; Livi, K. J.; Wang, C. *Nano Lett.* **2015**, *15*, 6829−6835.
(27) Xie, M. S.; Xia, B. Y.; Li, Y.; Yan, Y.; Yang, Y.; Sun, Q.; Chan, S. H.; Fisher, A.; Wang, X. *Energy Environ. Sci.* **2016**, *9*, 1687−1695.
(28) Feng, X.; Jiang, K.; Fan, S.; Kanan, M. W. *ACS Cent. Sci.* **2016**, *2*, 169−174.
(29) Cui, F.; Yu, Y.; Dou, L.; Sun, J.; Yang, Q.; Schildknecht, C.; Schierle-Arndt, K.; Yang, P. *Nano Lett.* **2015**, *15*, 7610−7615.
(30) Dou, L.; Cui, F.; Yu, Y.; Khanarian, G.; Eaton, S. W.; Yang, Q.; Resasco, J.; Schildknecht, C.; Schierle-Arndt, K.; Yang, P. *ACS Nano* **2016**, *10*, 2600−2606.
(31) Kuhl, K. P.; Cave, E. R.; Abram, D. N.; Jaramillo, T. F. *Energy Environ. Sci.* **2012**, *5*, 7050.
(32) Stankovich, S.; Dikin, D. A.; Piner, R. D.; Kohlhaas, K. A.; Kleinhammes, A.; Jia, Y.; Wu, Y.; Nguyen, S. T.; Ruoff, R. S. *Carbon* **2007**, *45*, 1558−1565.
(33) Chen, Z.; Zhang, X.; Lu, G. *Chem. Sci.* **2015**, *6*, 6829−6835.

DOI: 10.1021/acs.nanolett.6b05287
Nano Lett. 2017, 17, 1312−1317